Hyperparameter Tuning of EfficientNet Method for Optimization of Malaria Detection System Based on Red Blood Cell Image

Yuri Pamungkas [1]*, Dwinka Syafira Eljatin [2]

Department of Medical Technology, Institut Teknologi Sepuluh Nopember Surabaya [1],
Department of Medicine, Institut Teknologi Sepuluh Nopember Surabaya [2]
Surabaya, Indonesia
yuri@its.ac.id[1], dwinka@its.ac.id[2]

Abstract— **Nowadays, malaria has become an infectious disease with a high mortality rate. One way to detect malaria is through microscopic examination of blood preparations, which is done by experts and often takes a long time. With the development of deep learning technology, the observation of blood cell images infected with malaria can be more easily done. Therefore, this study proposes a red blood cell image-based malaria detection system using the EfficientNet method with hyperparameter tuning. There are three parameters which are learning rate, activation function, and optimiser. The learning rate used is 0.01 and 0.001, while the activation functions used are ReLU and Tanh. In addition, the optimisers used include Adam, SGD, and RMSProp. In the implementation, the cell image dataset from the NIH repository was pre-processed such as resizing, rotating, filtering, and data augmentation. Then the data is trained and tested on several EfficientNet models (B0, B1, B3, B5, and B7) and their performance values are compared. Based on the test results, EfficientNet-B5 and B7 models showed the best performance compared to other EfficientNet models. The most optimal system test results are when the EfficientNet B5 model is used with a learning rate of 0.001, ReLU activation function, and Adam optimiser, with values of 97.69% (accuracy), 98.36% (precision), and 97.03% (recall). This research has proven that proper model selection and hyperparameter tuning can maximise the performance of cell image-based malaria detection system. The development of this EfficientNet-based diagnostic method is more sensitive and specific in malaria detection using RBCs.**

Keywords— *Malaria Detection, Red Blood Cell Image, EfficientNet, Hyperparameter Tuning, Model Performance*

I. INTRODUCTION

In 2023, malaria remains a serious global health problem, with more than 249 million cases and approximately 619,000 deaths reported in the previous year. Sub-Saharan Africa is the most affected region, with more than 95% of all global cases and deaths occurring in this region [1]. Countries such as Nigeria, the Democratic Republic of Congo and Tanzania account for the majority of the malaria burden [2]. While prevention efforts such as the distribution of insecticide-treated bed nets and the introduction of the RTS,S/AS01 malaria vaccine have been implemented, significant challenges remain, including resistance to drugs and insecticides, as well as the impact of climate change exacerbating the situation [3]. There

are many challenges in malaria detection efforts. One of the main challenges in malaria detection is the reliability of the blood tests used for diagnosis. Although blood tests, such as Rapid Diagnostic Tests (RDTs) and microscopic examination [4-6], are the most commonly used methods, there are some significant challenges related to their accuracy and applicability in the field.

Microscopic examination, considered the gold standard, requires specialised expertise and adequate infrastructure, which is often not available in remote areas. In addition, factors such as blood sample quality, training of laboratory personnel, and equipment used can affect the accuracy of test results [7]. Rapid Diagnostic Tests (RDTs), which are easier to use and do not require a specialised laboratory, also face challenges regarding their sensitivity and specificity, especially in detecting infections with low parasitemia [8]. Parasite resistance to drugs can also affect test results, where resistant parasites may not be detected correctly [9]. In some areas, the accuracy of detecting resistant parasites is reduced because health workers may not be trained to use diagnostic tools correctly. The challenge of accurate and reliable methods to detect resistant malaria parasites is not properly recognised and can lead to delays in treatment and potentially increase the risk of death. Overcoming this challenge will require increased development of more sensitive and specific diagnostic methods, as well as increased access to more advanced technologies. These challenges point to the need for further research to develop more accurate and reliable detection methods, as well as improved infrastructure and training in areas most affected by malaria.

There have also been many studies related to Malaria detection based on red blood cell images (taken from microscope observations). Hemachandran, et al [10] proposed a machine learning-based malaria detection system on red blood smears. A total of 27,558 blood smear image data, consisting of 13,778 uninfected images and 13,780 infected images were used in this study. The models used include ResNet50, MobileNetV2, and CNN. As a result, the MobileNetV2 model was able to show the most optimal detection performance, with an accuracy rate of 97.06%. In addition to accuracy parameters, evaluation metrics such as precision, recall, f1-score, and ROC were also used to validate

the model test results. In their research, Mujahid et al [11] also proposed malaria detection based on Deep Learning EfficientNet. This model is considered capable of automatically extracting low- and high-level features in blood smear images to detect malaria parasites. In addition, K-Fold Cross Validation was also utilised to validate the results of the proposed model. As a result, the model has an accuracy rate of 97.57% in detecting malaria based on red blood smear images.

Asiya, et al [12] successfully proposed a malaria detection system using deep learning on infected and uninfected RBC image datasets. This dataset is obtained from the publicly accessible Kaggle Repository. The deep learning models used were CNN, Inception ResNet-v2, ResNet-101, Inception-v3, and VGG19. As a result, the ResNet-v2 model shows the best accuracy rate of 95.4%. The system proposed by Jameela et al [13] was also able to detect malaria quite accurately. Red blood smear images are used as input to CNN models such as ResNet34, ResNet50, VGG-16, and VGG-19 to detect Plasmodium parasites that cause malaria. In this study, the before and after fine-tuning results on test data using several models were compared. The results obtained the best accuracy rate reached 96.09% (before fine-tuning was applied) and 97.20% (after fine-tuning was applied) on the VGG19 model.

Based on several previous studies, this research will also propose a red blood cell smear-based malaria detection system using the EfficientNet model approach. The novelty of this study compared to previous studies is the use of hyperparameter tuning on several types of EfficientNet models for RBC-based malaria detection. Hyperparameter settings are performed on the learning rate, optimizer, and activation function of EfficientNet to obtain optimal detection system performance. The EfficientNet model has several types of architecture ranging from EfficientNet B0 to B7, where the higher the block (B) used, the more parameters will be generated. However, only EfficientNet B0, B1, B3, B5, and B7 are used in this study. The system performance will be observed based on its evaluation matrix value, such as accuracy, precision, and recall.

II. METHODOLOGY

This research uses the EfficientNet model approach to automatically distinguish red blood cell images infected with the parasite that causes Malaria. The EfficientNet model will work based on the hyperparameter settings on the architecture used. Therefore, to realise the red blood cell image-based malaria detection system, there are several steps that are carried out starting from collecting RBC data, pre-processing data, EfficientNet modelling, system testing, and model evaluation. Below is a flow chart of the research stages.
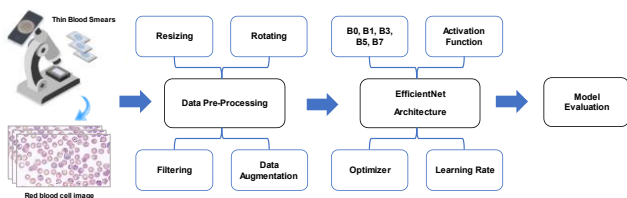

Figure 1. Methodology Research

A. Data Collection

This research uses red blood cell images infected with Plasmodium falciparum, which are stored in the National Institutes of Health (NIH) repository [14]. The Malaria RBC dataset from the National Institutes of Health (NIH) repository is one of the most widely used datasets in malaria detection research using machine learning and deep learning. This dataset contains thousands of microscopic images of red blood cells (RBCs) that have been classified into two main categories: red blood cells infected with malaria parasites and healthy red blood cells. A total of 27,560 images of red blood samples were used in this study (13,780 normal blood samples and 13,780 parasite-infected red blood samples). Each image was taken using an optical microscope and stained with a special dye to clarify the structure of the parasites in the red blood cells. This dataset is very important as it provides high-quality data that can be used to train and test machine learning models to detect malaria with high accuracy. The availability of clear annotations and a large amount of data allows the development of robust and reliable models for clinical applications. Below are some examples of normal and parasite-infected red blood cell image samples
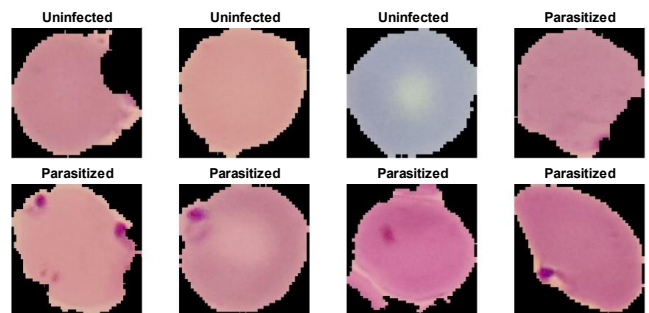

Figure 2. Red Blood Cell Image

B. . Data Pre-Processing

Resizing the red blood cell image for malaria detection is an important step in data pre-processing. Resizing changes the size of the image to suit the needs of deep learning models, which often require input images with specific dimensions [15]. By ensuring all images are of a consistent size, this process helps in standardising the data, allowing the model to analyse each image in a uniform manner without being compromised by size variations [16]. In addition, resizing also allows for more efficient use of memory and computation, which is important when handling large datasets [17]. Image rotation is a subset of data augmentation techniques that aims to increase the variety in a dataset without increasing the number of original images [18]. In the context of malaria detection, rotation can be applied to red blood cell images to simulate various cell orientations that may be encountered in real practice [19]. By rotating at different angles, the model is trained to recognise malaria parasites regardless of image orientation. This improves the robustness of the model and helps in overcoming the problem of overfitting by providing more data variations to learn from [20].

Filtering is a technique used to improve image quality by removing noise or disturbances that may obscure important features in red blood cell images [21]. Filters such as Gaussian

or median are often used to smooth the image, reduce noise, and retain relevant details [22]. In malaria detection, filtering helps to ensure that important features such as the shape and texture of red blood cells and the presence of parasites are clearly visible to the model [23]. Together with other data augmentation techniques such as resizing and rotating, filtering helps to create a cleaner and more variety-rich dataset, which ultimately improves the performance of the model in detecting malaria with higher accuracy [24].

C. EfficientNet Architecture

EfficientNet is a convolutional network architecture (CNN) introduced by Google AI to achieve a balance between performance and computational efficiency in computer vision tasks, such as image classification [25]. It is based on the simple yet effective idea of scaling the model proportionally in three main dimensions: depth, width, and resolution [26]. Unlike traditional approaches that only scale up one dimension, EfficientNet combines these three aspects using a method called "compound scaling," which results in significant performance improvements without requiring a large increase in the number of parameters [27]. EfficientNet achieves state-of-the-art performance in various benchmarks with a lower number of parameters and computation than previous models, making it a popular choice in applications that require high efficiency, such as mobile devices and edge computing [28].

EfficientNet consists of eight models, EfficientNet B0 to EfficientNet B7, built on the principle of compound scaling [29]. EfficientNet B0 is the base model in the series and serves as a starting point for the development of more complex models [30]. B0 is designed using the neural architecture search (NAS) technique, which automatically finds the optimal architecture with a minimal number of parameters and computation [31]. Despite being the smallest model in the series, B0 still demonstrates competitive performance across a wide range of computer vision tasks, making it ideal for applications that require high computational efficiency [32].

As the scale increases from EfficientNet B1 to B7, each model is optimised by incorporating proportional increases in depth, width and resolution. For example, B1 has more layers and neurons in each layer compared to B0, and processes images with higher resolution [33]. These improvements continue up to B7, which is the largest and most complex model in the series, with much higher depth, width, and resolution, allowing it to achieve very high accuracy on benchmarks such as ImageNet [34]. However, with the increased size and complexity, the B7 also requires more computing power and memory, making it more suitable for environments with larger computing resources, such as servers and data centres [35].

EfficientNet's success lies in its efficiency and scalability. Each model from B0 to B7 is designed to deliver the best performance under specific computing constraints, allowing users to choose the model that best suits their specific application needs [36]. If efficiency and power consumption are priorities, models such as B0 or B1 may be more suitable. On the other hand, if accuracy is the top priority and computational resources are not an issue, then models such as B6 or B7 could be the right choice [37]. Thus, the EfficientNet architecture

provides a flexible solution for various needs in image recognition and computer vision tasks.

The most fundamental part of a neural network is the stem, followed by the construction of the architecture starting with the eight blocks and then the final layers [38]. Each block is composed of several sub-blocks (modules) that vary and continue to grow from EfficientNet-B0 to EfficientNet-B7 [39]. The architecture of the stem, final layers, and sub-block is shown in the following figure.
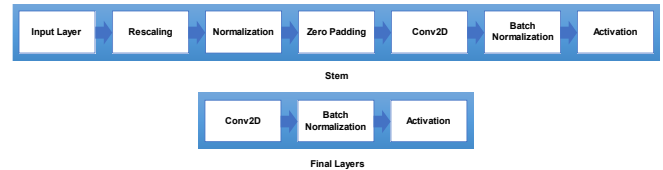

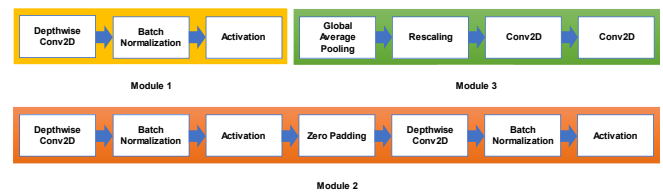*Figure 3. EfficientNet Stem and Final Layers Architecture*

Figure 4.Sub-block Architecture of EfficientNet

Each component (stem, final layers, and sub-blocks) has a specific role in image processing and feature learning, which ultimately allows the model to achieve optimal results in various computer vision tasks [40]. The stem function in EfficientNet is the initial part of the network that is responsible for processing the raw image input into an initial feature representation that can be processed by the deeper network [41]. Typically, this stem function consists of an initial convolutional layer that has filters of large size (e.g. 3x3) and stride greater than 1, which aims to reduce the spatial dimension of the input image while extracting basic features such as edges, texture, and simple patterns [42]. This stem function helps to simplify the raw image into a more compact feature representation, which will then be further processed by subsequent blocks in the network [43].

Sub-blocks in EfficientNet are the main processing units consisting of multiple convolutional layers and other non-linear operations, such as batch normalisation and activation functions (e.g., ReLU or Swish) [44]. These sub-blocks are based on the Mobile Inverted Bottleneck Convolution (MBConv) adapted from the MobileNetV2 architecture. Each sub-block serves to extract and learn more complex features from the input image through a series of efficient convolutional operations [45]. MBConv utilises a depthwise separable convolution technique, which separates spatial and channel convolutions, thus reducing the number of parameters and computation without compromising accuracy. Sub-blocks are also often equipped with squeeze-and-excitation (SE) modules, which help the model to attend to important features by reweighting channels based on their relevance to the task at hand [46].

The final layers in EfficientNet are the last layers of the network that are responsible for condensing the features learnt throughout the network into outputs that are suitable for a particular task, such as classification or object detection [47]. Typically, these final layers consist of global average pooling that reduces the spatial dimension of the feature map to a one-dimensional vector, followed by a fully connected layer that generates the final prediction [48]. At this stage, the information that has been processed by the entire network is synthesised into a final decision, such as a class label in the case of image classification [49]. These final layers are designed to combine all the previously learnt features in an optimal way, so that the model can produce output with high accuracy. With the combination of stem functions for initial feature extraction, sub-blocks for complex and efficient feature learning, and final layers for final decision making, EfficientNet is able to achieve high performance with significant computational efficiency [50]. Each of these components is designed to work together harmoniously, ensuring that the model can process images quickly and accurately in various computer vision applications [51].

D. Hyperparameter Tuning and Model Evaluation

To optimise EfficientNet's performance, hyperparameter tuning can include adjustments to these scale factors, such as the scaling coefficient which determines how large the model is scaled up or down, as well as other hyperparameters such as learning rate, batch size, and regularization [52]. This tuning process is important to find the right balance between accuracy and computational efficiency, as EfficientNet is designed to deliver superior performance with lower computational resources than other larger models [53]. In this research, hyperparameter tuning is performed by varying the type of activation function and optimiser used by the EfficientNet model. In addition, the learning rate was also changed to see the performance of the model. The following are the hyperparameter tuning scenarios on the EfficientNet model tested in the study.

TABLE I. HYPERPARAMETER TUNING ON THE EFFICIENTNET MODEL

Model EfficientNet	B0, B1, B3, B5, B7
Epoch	15
Optimizer	SGD, Adam, RMSProp
Learning Rate	0.01, 0.001
Activation Function	ReLU, Tanh

In addition, model evaluation is also conducted to measure the performance of EfficientNet. This evaluation is usually done using certain metrics such as accuracy, precision, and recall to measure how well the model is able to detect results on data that has never been seen before (validation data or test set).

$$Accuracy = \frac{TP + TN}{TP + FP + FN + TN} \quad (1)$$

$$Precision = \frac{TP}{TP + FP} \quad (2)$$

$$Recall = \frac{TP}{TP + FN} \quad (3)$$

Accuracy measures the percentage of correct predictions out of all predictions, giving a general idea of model performance, but can be misleading on unbalanced datasets. Precision measures the precision of positive predictions, i.e. how many positive predictions are correct compared to all positive predictions made, important when false positives are to be minimised. Recall, on the other hand, measures the sensitivity of the model or its ability to detect all true positive instances, crucial when not missing positive predictions is a priority. These three metrics are often used together to provide a deeper understanding of the model's performance in various contexts.

III. RESULTS AND DISCUSSION

This research aims to obtain a red blood cell image-based malaria detection model that has optimal system performance. Therefore, several EfficientNet architectures (B0, B1, B3, B5, and B7) are proposed in this study. Each EfficientNet architecture is then tuned with hyperparameters by changing the learning rate (0.01 and 0.001), activation function type (ReLU and Tanh), and optimiser type (Adam, SGD, and RMSProp). Based on the results of hyperparameter tuning and model testing, the performance metrics are obtained as shown in the following table.

TABLE II. PERFORMANCE METRICS OF EFFICIENTNET MODEL WITH LEARNING RATE = 0.01 AND ACTIVATION FUNCTION = RELU

Optimizer	Model	Accuracy	Precision	Recall
Adam	B0	94.69	97.78	91.52
	B1	94.97	98.17	91.72
	B3	95.65	98.75	92.53
	B5	**96.73**	**98.24**	**95.23**
	B7	96.24	98.67	93.79
SGD	B0	94.47	97.59	91.26
	B1	94.69	97.79	91.53
	B3	95.37	98.56	92.18
	B5	**96.51**	**97.87**	**95.13**
	B7	95.96	98.39	93.51
RMSProp	B0	94.33	97.31	91.25
	B1	94.60	97.78	91.36
	B3	95.28	98.27	92.25
	B5	**96.42**	**97.78**	**95.05**
	B7	96.10	98.58	93.62

Table 2 shows the performance metrics of EfficientNet B0 to B7 with learning rate 0.01 and ReLU activation function. When the optimiser used is Adam (Adaptive Moment Estimation), the Efficient B5 model shows accuracy, precision and recall rates of 96.73%, 98.24% and 95.23%. Similarly, when the optimiser used was SGD (Stochastic Gradient Descent), EfficientNet B5 showed performance values of 96.51% (accuracy), 97.87% (precision), and 95.13% (recall). Another optimiser, RMSProp (Root Mean Square Propagation) was also used in testing this model (EfficientNet B5). As a result, the accuracy, precision, and recall values from system testing reached 96.42%, 97.78%, and 95.05%. So EfficientNet B5 is the most optimal model compared to other EfficientNet models, when setting the learning rate = 0.01 and the activation function is ReLU.

TABLE III. PERFORMANCE METRICS OF EFFICIENTNET MODEL WITH LEARNING RATE = 0.001 AND ACTIVATION FUNCTION = RELU

Optimizer	Model	Accuracy	Precision	Recall
Adam	B0	96.83	97.19	96.49
	B1	97.23	98.08	96.40
	B3	97.01	97.63	96.40
	B5	**97.69**	**98.36**	**97.03**
	B7	97.60	98.00	97.21
SGD	B0	96.46	96.83	96.13
	B1	97.05	97.80	96.31
	B3	96.87	97.54	96.22
	B5	**97.51**	**98.26**	**96.76**
	B7	97.46	97.82	97.12
RMSProp	B0	96.05	96.38	95.77
	B1	96.83	97.62	96.04
	B3	96.73	97.53	95.96
	B5	97.41	97.91	96.93
	B7	**97.46**	**97.91**	**97.03**

Table 3 shows the performance metrics of EfficientNet B0 to B7 with learning rate 0.001 and activation function ReLU. When the optimiser used is Adam, the Efficient B5 model shows accuracy, precision and recall rates of 97.69%, 98.36% and 97.03%, respectively. Similarly, when the optimiser used was SGD, EfficientNet B5 showed performance values of 97.51% (accuracy), 98.26% (precision), and 96.76% (recall). However, when the optimiser used is RMSProp, EfficientNet B7 shows the optimal performance values, namely 97.46%, 97.91%, and 97.03%. In general, from the results of system testing, it can be seen that there is an increase in the performance value of accuracy, precision, and recall when the learning rate is changed from the previous 0.01 to 0.001.

TABLE IV. PERFORMANCE METRICS OF EFFICIENTNET MODEL WITH LEARNING RATE = 0.01 AND ACTIVATION FUNCTION = TANH

Optimizer	Model	Accuracy	Precision	Recall
Adam	B0	93.61	95.92	91.16
	B1	94.01	96.38	91.49
	B3	94.74	97.23	92.13
	B5	**95.74**	**97.29**	**94.12**
	B7	95.42	97.36	93.39
SGD	B0	93.24	95.26	91.03
	B1	93.65	95.90	91.21
	B3	94.51	96.85	92.03
	B5	**95.51**	**96.92**	**94.03**
	B7	95.24	97.17	93.21
RMSProp	B0	93.33	95.36	91.13
	B1	93.74	96.18	91.14
	B3	94.51	97.13	91.77
	B5	**95.60**	**97.10**	**94.03**
	B7	95.24	97.17	93.21

Table 4 shows EfficientNet performance metrics from B0 to B7 with a learning rate of 0.01 and a Tanh activation function. When the optimizer used is Adam, the Efficiant B5 model showed accuracy, precision, and recall levels of 95.74%, 97.29%, and 94.12%. Similarly, when the optimiser used is SGD, EffizientNet B5 showed optimal performance values of 96.51% (accuracy), 96.92% (precision), and 94.03% (recall). The RMSProp Optimizer used in this study reached system performance levels (accuracy, precision, and recalls) of 95,60%, 97,10% and 94,03%. Thus, EfficientNet B5 is the most optimal model compared to the other EfficentNet models, when learning rate settings = 0.01, and activation functions are Tanh. This feature is similar to testing the system model when the system function is activated by ReLU with its learning rate 0.01.

TABLE V. PERFORMANCE METRICS OF EFFICIENTNET MODEL WITH LEARNING RATE = 0.001 AND ACTIVATION FUNCTION = TANH

Optimizer	Model	Accuracy	Precision	Recall
Adam	B0	95.42	95.89	94.94
	B1	96.05	96.52	95.55
	B3	96.42	96.90	95.94
	B5	97.28	97.81	96.75
	B7	**97.28**	**97.73**	**96.84**
SGD	B0	95.06	95.61	94.48
	B1	95.78	96.25	95.29
	B3	96.15	96.63	95.67
	B5	**97.01**	**97.53**	**96.48**
	B7	96.96	97.45	96.49
RMSProp	B0	95.15	95.62	94.67
	B1	95.78	96.16	95.37
	B3	96.10	96.63	95.59
	B5	97.01	97.54	96.48
	B7	**97.10**	**97.63**	**96.57**

Table 5 shows the performance metrics of EfficientNet B0 to B7 with a learning rate of 0.001 and a Tanh activation function. When the optimizer used is Adam, the Efficient B7 model shows accuracy, precision, and recall levels reaching 97.28%, 97.73%, and 96.84%. However, when the optimizer used is SGD, the EfficientNet B5 model shows optimal performance values of 97.01% (accuracy), 97.53% (precision), and 96.48% (recall). When the optimizer used is RMSProp, EfficientNet B7 shows optimal performance values of 97.10%, 97.63%, and 96.57%. From these results, it can be seen that the EfficientNet B7 model tends to be dominant when testing the system using a learning rate of 0.001 and the Tanh activation

function.

In general, it can be seen that the optimal performance of the malaria detection system occurs when testing using EfficientNet models B5 and B7. EfficientNet B5 and B7 are better at malaria cell image detection compared to smaller variants such as B0, B1, and B3 because they have a more complex architecture and greater capacity to capture fine and important features in the image. Malaria cell images often have very fine microscopic details that are difficult to detect, such as small differences in cell shape or colour that indicate infection. Models such as B5 and B7, with greater input depth, width and resolution, are able to extract and process visual information more accurately and thoroughly, allowing them to recognise patterns and anomalies that smaller models may miss [54]. This results in better detection performance, with higher accuracy and sensitivity, which is especially important in medical applications where detection errors can have serious consequences. However, this improvement in accuracy comes at a higher computational cost. When further analysed, the smaller learning rate in training the EfficientNet model can have a significant effect on the model's performance. This can be seen from the increase in accuracy, precision and recall values when the learning rate is set smaller than before. A small learning rate makes the weight update at each iteration smoother and more careful, which can help the model achieve a more stable convergence and prevent the model from jumping past the minimum loss on the loss function landscape [55]. However, this also means that the training process will take longer, as more iterations are required to achieve convergence.

Another parameter, the activation function jg has an influence on the performance of the model. The ReLU activation function tends to be more effective than the Tanh function in improving the accuracy, precision and recall values of the EfficientNet-based malaria detection system. ReLU activation function is better in malaria cell image detection compared to Tanh activation function because ReLU overcomes some of the problems that often occur in Tanh, especially related to vanishing gradient. ReLU only maps negative input values to zero and keeps positive values as they are, which allows the gradient to remain large and stable during training, even in deep neural networks such as those often used in medical image detection [56]. This is important in tasks such as malaria cell detection, where small and complex details in the image must be accurately identified. While Tanh, which maps inputs to the range [-1, 1], tends to have a small gradient on inputs close to the upper or lower boundary, causing learning to be slow or even stalled in the deepest layers [57]. With ReLU, the model can learn more quickly and efficiently, enabling sharper feature detection and responsiveness to variations in malaria cell images, ultimately improving detection accuracy and reliability.

In addition, the use of different optimisers in the EfficientNet model made a significant difference to the performance of the system. The Adam optimiser provides improved accuracy, precision and recall values compared to the SGD and RMSProp optimisers in cell image-based malaria detection. Adam is better because it is able to provide a balance between convergence speed and training stability. Adam uses adaptive learning rates and momentum, which allows the model to dynamically adjust weight updates based on the mean gradient and variance of previous iterations [58]. This is particularly useful in tasks such as malaria cell image detection, where images have complex variations and the model requires efficient learning of subtle features in the data. Compared to SGD, which tends to be slow and prone to getting stuck at a local minimum, Adam tends to achieve convergence faster and more accurately without requiring much hyperparameter adjustment [59]. While RMSProp also uses adaptive learning rates, Adam is superior because it utilises momentum to accelerate training in the right direction and reduce oscillations [60]. With Adam, the model can better capture microscopic details in malaria cell images, which is important for improving diagnosis accuracy and early detection of the disease.

IV. CONCLUSION

In this study, researchers implemented the EfficientNet B0 to B7 models to detect malaria based on red blood cell images. The data used came from the National Institutes of Health repository and is publicly accessible. In addition, to obtain an optimal model, hyperparameter tuning was carried out in the form of learning rate, activation function, and optimizer on EfficientNet. The learning rates used were 0.01 and 0.001, while the activation functions were ReLU and Tanh. The EfficientNet optimizers used were Adam, SGD, and RMSProp. To measure the performance level of each model, researchers used several evaluation parameters such as accuracy, precision, and recall. Based on the test results, the EfficientNet-B5 and B7 models showed the best performance compared to other EfficientNet models. The most optimal system test results are when the model used is EfficientNet B5 with a learning rate of 0.001, ReLU activation function, and Adam optimizer. This study has proven that the selection of the right model and hyperparameter settings can maximize the performance of the cell image-based malaria detection system. The use of EfficientNet in RBC-based malaria detection has several advantages such as accelerating the parasite detection process, reducing the involvement of medical personnel who are often biased, and minimizing human error in interpretation. Resistant malaria parasites can also be detected well because the EfficientNet model is able to remember the parasite image pattern in RBC well, this can be seen from its performance value which reaches 97.69% (for accuracy), 98.36% (for precision), and 97.03% (for recall). However, this study has not yet discussed and considered the computation time of the EfficientNet model in the malaria detection process. Although the EfficientNet model with high blocks such as B5 and B7 has better performance than the blocks below (B0, B1, and B3), the computation time is quite long. So in future research, researchers will focus on the computation time in using the detection model. So that the accuracy can still be increased but the computation time can be more efficient.

scheme of the PPHKI 2024.

REFERENCES

[1] P. Venkatesan, "The 2023 WHO World malaria report," The Lancet Microbe, vol. 5, no. 3, Jan. 2024, doi: https://doi.org/10.1016/s2666-5247(24)00016-8.

[2] C. Marston et al., "Developing the Role of Earth Observation in Spatio-Temporal Mosquito Modelling to Identify Malaria Hot-Spots," Remote Sensing, vol. 15, no. 1, pp. 43–43, Dec. 2022, doi: https://doi.org/10.3390/rs15010043.

[3] H. Sutanto, "Combating Malaria with Vaccines: Insights from the One Health Framework," Deleted Journal, vol. 69, no. 3, pp. 153–166, Jul. 2024, doi: https://doi.org/10.3390/amh69030015.

[4] F. Grignaffini, P. Simeoni, A. Alisi, and F. Frezza, "Computer-Aided Diagnosis Systems for Automatic Malaria Parasite Detection and Classification: A Systematic Review," Electronics, vol. 13, no. 16, pp. 3174–3174, Aug. 2024, doi: https://doi.org/10.3390/electronics13163174.

[5] T. Song, Y. Wang, Y. Li, and G. Fan, "A Mathematical Analysis of Competitive Dynamics and Aggressive Treatment in the Evolution of Drug Resistance in Malaria Parasites," Mathematics, vol. 12, no. 10, pp. 1595–1595, May 2024, doi: https://doi.org/10.3390/math12101595.

[6] A. Alsulimani et al., "The Impact of Artificial Intelligence on Microbial Diagnosis," Microorganisms, vol. 12, no. 6, pp. 1051–1051, May 2024, doi: https://doi.org/10.3390/microorganisms12061051.

[7] D. A. Deo, E. H. Herningtyas, U. S. Intansari, T. M. Perdana, E. H. Murhandarwati, and M. H. N. E. Soesatyo, "Difference between Microscopic and PCR Examination Result for Malaria Diagnosis and Treatment Evaluation in Sumba Barat Daya, Indonesia," Tropical Medicine and Infectious Disease, vol. 7, no. 8, pp. 153–153, Jul. 2022, doi: https://doi.org/10.3390/tropicalmed7080153.

[8] D. G. Mordue et al., "Plasma Blood Levels of Tafenoquine following a Single Oral Dosage in BALBc Mice with Acute Babesia microti Infection That Resulted in Rapid Clearance of Microscopically Detectable Parasitemia," Pathogens, vol. 12, no. 9, pp. 1113–1113, Aug. 2023, doi: https://doi.org/10.3390/pathogens12091113.

[9] S. Abd El-Ghany, M. Elmogy, and A. El-Aziz, "Computer-Aided Diagnosis System for Blood Diseases Using EfficientNet-B3 Based on a Dynamic Learning Algorithm," Diagnostics, vol. 13, no. 3, p. 404, Jan. 2023, doi: https://doi.org/10.3390/diagnostics13030404.

[10] K. Hemachandran et al., "Performance Analysis of Deep Learning Algorithms in Diagnosis of Malaria Disease," Diagnostics, vol. 13, no. 3, p. 534, Jan. 2023, doi: https://doi.org/10.3390/diagnostics13030534.

[11] M. Mujahid et al., "Efficient deep learning-based approach for malaria detection using red blood cell smears," Scientific Reports, vol. 14, no. 1, p. 13249, Jun. 2024, doi: https://doi.org/10.1038/s41598-024-63831-0.

[12] S. Asiya, D. Aparna, N. Mahender, M. Raamizuddin, and P. Anoosha, "Malaria Parasite Detection Using Deep Neural Networks," Lecture notes in networks and systems, pp. 309–321, Jan. 2024, doi: https://doi.org/10.1007/978-981-99-7817-5_23.

[13] T. Jameela, K. Athotha, N. Singh, V. K. Gunjan, and S. Kahali, "Deep Learning and Transfer Learning for Malaria Detection," Computational Intelligence and Neuroscience, vol. 2022, pp. 1–14, Jun. 2022, doi: https://doi.org/10.1155/2022/2221728.

[14] Y. M. Kassim et al., "Clustering-Based Dual Deep Learning Architecture for Detecting Red Blood Cells in Malaria Diagnostic Smears," IEEE Journal of Biomedical and Health Informatics, pp. 1–1, 2020, doi: https://doi.org/10.1109/jbhi.2020.3034863.

[15] L. Alzubaidi, M. A. Fadhel, O. Al-Shamma, J. Zhang, and Y. Duan, "Deep Learning Models for Classification of Red Blood Cells in Microscopy Images to Aid in Sickle Cell Anemia Diagnosis," Electronics, vol. 9, no. 3, p. 427, Mar. 2020, doi: https://doi.org/10.3390/electronics9030427.

[16] K. Hoyos and W. Hoyos, "Supporting Malaria Diagnosis Using Deep Learning and Data Augmentation," Diagnostics, vol. 14, no. 7, p. 690, Jan. 2024, doi: https://doi.org/10.3390/diagnostics14070690.

[17] R. Nakasi, E. Mwebaze, and A. Zawedde, "Mobile-Aware Deep Learning Algorithms for Malaria Parasites and White Blood Cells Localization in Thick Blood Smears," Algorithms, vol. 14, no. 1, p. 17, Jan. 2021, doi: https://doi.org/10.3390/a14010017.

[18] K. M. F. Fuhad, J. F. Tuba, Md. R. A. Sarker, S. Momen, N. Mohammed, and T. Rahman, "Deep Learning Based Automatic Malaria Parasite Detection from Blood Smear and Its Smartphone Based Application," Diagnostics, vol. 10, no. 5, May 2020, doi: https://doi.org/10.3390/diagnostics10050329.

[19] Y. S. Cho and P. C. Hong, "Applying Machine Learning to Healthcare Operations Management: CNN-Based Model for Malaria Diagnosis," Healthcare, vol. 11, no. 12, p. 1779, Jan. 2023, doi: https://doi.org/10.3390/healthcare11121779.

[20] R. Ali, R. C. Hardie, B. N. Narayanan, and T. M. Kebede, "IMNets: Deep Learning Using an Incremental Modular Network Synthesis Approach for Medical Imaging Applications," Applied Sciences, vol. 12, no. 11, p. 5500, May 2022, doi: https://doi.org/10.3390/app12115500.

[21] Y. Dong and W. David Pan, "Image Classification in JPEG Compression Domain for Malaria Infection Detection," Journal of Imaging, vol. 8, no. 5, pp. 129–129, May 2022, doi: https://doi.org/10.3390/jimaging8050129.

[22] A. Kareem, H. Liu, and Vladan Velisavljevic, "A Privacy-Preserving Approach to Effectively Utilize Distributed Data for Malaria Image Detection," Bioengineering, vol. 11, no. 4, pp. 340–340, Mar. 2024, doi: https://doi.org/10.3390/bioengineering11040340.

[23] M. Semakula, F. Niragire, and C. Faes, "Spatio-Temporal Bayesian Models for Malaria Risk Using Survey and Health Facility Routine Data in Rwanda," International journal of environmental research and public health/International journal of environmental research and public health, vol. 20, no. 5, pp. 4283–4283, Feb. 2023, doi: https://doi.org/10.3390/ijerph20054283.

[24] S. Paul, S. Batra, K. Mohiuddin, Mohamed Nadhmi Miladi, D. Anand, and O. A. Nasr, "A Novel Ensemble Weight-Assisted Yolov5-Based Deep Learning Technique for the Localization and Detection of Malaria Parasites," Electronics, vol. 11, no. 23, pp. 3999–3999, Dec. 2022, doi: https://doi.org/10.3390/electronics11233999.

[25] S. Gamil, F. Zeng, Moath Alrifaey, M. Asim, and N. Ahmad, "An Efficient AdaBoost Algorithm for Enhancing Skin Cancer Detection and Classification," Algorithms, vol. 17, no. 8, pp. 353–353, Aug. 2024, doi: https://doi.org/10.3390/a17080353.

[26] I. Manole, A.-I. Butacu, R. N. Bejan, and G.-S. Tiplica, "Enhancing Dermatological Diagnostics with EfficientNet: A Deep Learning Approach," Bioengineering, vol. 11, no. 8, pp. 810–810, Aug. 2024, doi: https://doi.org/10.3390/bioengineering11080810.

[27] K. Arai, J. Shimazoe, and M. Oda, "A Method for Maintaining a Unique Kurume Kasuri Pattern of Woven Textile Classified by EfficientNet by Means of LightGBM-Based Prediction of Misalignments," Information, vol. 15, no. 8, pp. 434–434, Jul. 2024, doi: https://doi.org/10.3390/info15080434.

[28] Y.-H. Kao and C.-L. Lin, "Enhancing Diabetic Retinopathy Detection Using Pixel Color Amplification and EfficientNetV2: A Novel Approach for Early Disease Identification," Electronics, vol. 13, no. 11, pp. 2070–2070, May 2024, doi: https://doi.org/10.3390/electronics13112070.

[29] C.-Y. Lin et al., "Precision Identification of Locally Advanced Rectal Cancer in Denoised CT Scans Using EfficientNet and Voting System Algorithms," Bioengineering, vol. 11, no. 4, p. 399, Apr. 2024, doi: https://doi.org/10.3390/bioengineering11040399.

[30] M. A. Kiflie, D. P. Sharma, M. A. Haile, and R. Srinivasagan, "EfficientNet Ensemble Learning: Identifying Ethiopian Medicinal Plant Species and Traditional Uses by Integrating Modern Technology with Ethnobotanical Wisdom," Computers, vol. 13, no. 2, pp. 38–38, Jan. 2024, doi: https://doi.org/10.3390/computers13020038.

[31] W. Wang, X. Jiang, H. Yuan, J. Chen, X. Wang, and Z. Huang, "Research on Algorithm for Authenticating the Authenticity of Calligraphy Works Based on Improved EfficientNet Network," Applied Sciences, vol. 14, no. 1, pp. 295–295, Dec. 2023, doi: https://doi.org/10.3390/app14010295.

[32] C. I. Suciu, A. Marginean, V.-I. Suciu, G. A. Muntean, and S. D. Nicoară,

"Diabetic Macular Edema Optical Coherence Tomography Biomarkers Detected with EfficientNetV2B1 and ConvNeXt," Diagnostics, vol. 14, no. 1, pp. 76–76, Dec. 2023, doi: https://doi.org/10.3390/diagnostics14010076.

[33] M. Chekroun, Y. Mourchid, I. Bessières, and A. Lalande, "Deep Learning Based on EfficientNet for Multiorgan Segmentation of Thoracic Structures on a 0.35 T MR-Linac Radiation Therapy System," Algorithms, vol. 16, no. 12, pp. 564–564, Dec. 2023, doi: https://doi.org/10.3390/a16120564.

[34] H. Farman, M. M. Nasralla, S. B. A. Khattak, and B. Jan, "Efficient Fire Detection with E-EFNet: A Lightweight Deep Learning-Based Approach for Edge Devices," Applied Sciences, vol. 13, no. 23, p. 12941, Jan. 2023, doi: https://doi.org/10.3390/app132312941.

[35] H. N. Huynh, N. An, A. T. Tran, V. C. Nguyen, and T. N. Tran, "Classification of Breast Cancer Using Radiological Society of North America Data by EfficientNet," Nov. 2023, doi: https://doi.org/10.3390/engproc2023055006.

[36] Q. Abbas, Y. Daadaa, U. Rashid, M. Z. Sajid, and Mostafa, "HDR-EfficientNet: A Classification of Hypertensive and Diabetic Retinopathy Using Optimize EfficientNet Architecture," Diagnostics, vol. 13, no. 20, pp. 3236–3236, Oct. 2023, doi: https://doi.org/10.3390/diagnostics13203236.

[37] X. Li, X. Li, B. Han, S. Wang, and K. Chen, "Application of EfficientNet and YOLOv5 Model in Submarine Pipeline Inspection and a New Decision-Making System," Water, vol. 15, no. 19, pp. 3386–3386, Sep. 2023, doi: https://doi.org/10.3390/w15193386.

[38] Z. Liu, W. Sun, S. Chang, K. Zhang, Y. Ba, and R. Jiang, "Corn Harvester Bearing Fault Diagnosis Based on ABC-VMD and Optimized EfficientNet," Entropy, vol. 25, no. 9, pp. 1273–1273, Aug. 2023, doi: https://doi.org/10.3390/e25091273.

[39] L. Huang, Q. Tian, B.-H. Tang, W. Le, M. Wang, and X. Ma, "Siam-EMNet: A Siamese EfficientNet–MANet Network for Building Change Detection in Very High-Resolution Images," Remote Sensing, vol. 15, no. 16, pp. 3972–3972, Aug. 2023, doi: https://doi.org/10.3390/rs15163972.

[40] S. Chen et al., "Improving Patient Safety in the X-ray Inspection Process with EfficientNet-Based Medical Assistance System," Healthcare, vol. 11, no. 14, pp. 2068–2068, Jul. 2023, doi: https://doi.org/10.3390/healthcare11142068.

[41] N. Sharma, S. Gupta, M. Saleh, A. Sulaiman, Hani Alshahrani, and A. Shaikh, "EfficientNetB0 cum FPN Based Semantic Segmentation of Gastrointestinal Tract Organs in MRI Scans," Diagnostics, vol. 13, no. 14, pp. 2399–2399, Jul. 2023, doi: https://doi.org/10.3390/diagnostics13142399.

[42] F. Rajeena P. P. , A. S. U., M. A. Moustafa, and M. A. S. Ali, "Detecting Plant Disease in Corn Leaf Using EfficientNet Architecture—An Analytical Approach," Electronics, vol. 12, no. 8, p. 1938, Jan. 2023, doi: https://doi.org/10.3390/electronics12081938.

[43] T. Nazir, M. M. Iqbal, S. Jabbar, A. Hussain, and M. Albathan, "EfficientPNet—An Optimized and Efficient Deep Learning Approach for Classifying Disease of Potato Plant Leaves," Agriculture, vol. 13, no. 4, pp. 841–841, Apr. 2023, doi: https://doi.org/10.3390/agriculture13040841.

[44] Q. Dai et al., "Citrus Disease Image Generation and Classification Based on Improved FastGAN and EfficientNet-B5," Agronomy, vol. 13, no. 4, p. 988, Apr. 2023, doi: https://doi.org/10.3390/agronomy13040988.

[45] Z. Huang, L. Su, J. Wu, and Y. Chen, "Rock Image Classification Based on EfficientNet and Triplet Attention Mechanism," Applied Sciences, vol. 13, no. 5, p. 3180, Jan. 2023, doi: https://doi.org/10.3390/app13053180.

[46] M. Vijayan and V. S, "A Regression-Based Approach to Diabetic Retinopathy Diagnosis Using Efficientnet," Diagnostics, vol. 13, no. 4, p. 774, Feb. 2023, doi: https://doi.org/10.3390/diagnostics13040774.

[47] S. B. Punuri et al., "Efficient Net-XGBoost: An Implementation for Facial Emotion Recognition Using Transfer Learning," Mathematics, vol. 11, no. 3, p. 776, Feb. 2023, doi: https://doi.org/10.3390/math11030776.

[48] M. M. A. Rahhal, Y. Bazi, R. M. Jomaa, M. Zuair, and F. Melgani, "Contrasting EfficientNet, ViT, and gMLP for COVID-19 Detection in Ultrasound Imagery," Journal of Personalized Medicine, vol. 12, no. 10, p. 1707, Oct. 2022, doi: https://doi.org/10.3390/jpm12101707.

[49] B. Hu, J. Tang, J. Wu, and J. Qing, "An Attention EfficientNet-Based Strategy for Bearing Fault Diagnosis under Strong Noise," Sensors, vol. 22, no. 17, p. 6570, Jan. 2022, doi: https://doi.org/10.3390/s22176570.

[50] B. Li, B. Liu, S. Li, and H. Liu, "An Improved EfficientNet for Rice Germ Integrity Classification and Recognition," Agriculture, vol. 12, no. 6, p. 863, Jun. 2022, doi: https://doi.org/10.3390/agriculture12060863.

[51] N. Baghdadi, A. S. Maklad, A. Malki, and M. A. Deif, "Reliable Sarcoidosis Detection Using Chest X-rays with EfficientNets and Stain-Normalization Techniques," Sensors, vol. 22, no. 10, pp. 3846–3846, May 2022, doi: https://doi.org/10.3390/s22103846.

[52] M. Saleh et al., "Detection of Pneumonia from Chest X-ray Images Utilizing MobileNet Model," Healthcare, vol. 11, no. 11, pp. 1561–1561, May 2023, doi: https://doi.org/10.3390/healthcare11111561.

[53] A. M. Qadri, A. Raza, F. Eid, and L. Abualigah, "A novel transfer learning-based model for diagnosing malaria from parasitized and uninfected red blood cell images," Decision Analytics Journal, vol. 9, p. 100352, Dec. 2023, doi: https://doi.org/10.1016/j.dajour.2023.100352.

[54] Z. Zhu, S. Wang, and Y. Zhang, "ROENet: A ResNet-Based Output Ensemble for Malaria Parasite Classification," Electronics, vol. 11, no. 13, p. 2040, Jun. 2022, doi: https://doi.org/10.3390/electronics11132040.

[55] G. R. Mudavadkar et al., "Gastric Cancer Detection with Ensemble Learning on Digital Pathology: Use Case of Gastric Cancer on GasHisSDB Dataset," Diagnostics, vol. 14, no. 16, pp. 1746–1746, Aug. 2024, doi: https://doi.org/10.3390/diagnostics14161746.

[56] V. Sureshkumar, R. Sharma, S. Balasubramaniam, D. Jagannathan, J. Daniel, and S. Dhanasekaran, "Breast Cancer Detection and Analytics Using Hybrid CNN and Extreme Learning Machine," Journal of Personalized Medicine, vol. 14, no. 8, pp. 792–792, Jul. 2024, doi: https://doi.org/10.3390/jpm14080792.

[57] S. Bouguezzi, H. B. Fredj, T. Belabed, C. Valderrama, H. Faiedh, and C. Souani, "An Efficient FPGA-Based Convolutional Neural Network for Classification: Ad-MobileNet," Electronics, vol. 10, no. 18, p. 2272, Sep. 2021, doi: https://doi.org/10.3390/electronics10182272.

[58] H. Sun et al., "An Improved Medical Image Classification Algorithm Based on Adam Optimizer," Mathematics, vol. 12, no. 16, pp. 2509–2509, Aug. 2024, doi: https://doi.org/10.3390/math12162509.

[59] N. F. Alhussainan, B. Ben Youssef, and M. M. Ben Ismail, "A Deep Learning Approach for Brain Tumor Firmness Detection Based on Five Different YOLO Versions: YOLOv3–YOLOv7," Computation, vol. 12, no. 3, p. 44, Mar. 2024, doi: https://doi.org/10.3390/computation12030044.

[60] D. Lopez-Betancur et al., "Evaluation of Optimization Algorithms for Measurement of Suspended Solids," Water, vol. 16, no. 13, pp. 1761–1761, Jun. 2024, doi: https://doi.org/10.3390/w16131761.